

Neutron scattering study of $\text{PbMg}_{1/3}\text{Ta}_{2/3}\text{O}_3$ and $\text{BaMg}_{1/3}\text{Ta}_{2/3}\text{O}_3$ complex perovskites

S.N. Gvasaliya*

Laboratory for Neutron Scattering ETHZ & Paul-Scherrer Institut CH-5232 Villigen PSI Switzerland

B. Roessli and D. Sheptyakov

Laboratory for Neutron Scattering ETHZ & Paul-Scherrer Institut CH-5232 Villigen PSI, Switzerland

S.G. Lushnikov and T.A. Shaplygina

Ioffe Physical Technical Institute, 26 Politechnicheskaya, 194021, St. Petersburg, Russia

(Dated: May 25, 2020)

Neutron scattering investigations were carried out in $\text{PbMg}_{1/3}\text{Ta}_{2/3}\text{O}_3$ and $\text{BaMg}_{1/3}\text{Ta}_{2/3}\text{O}_3$ complex perovskites. The crystal structure of both compounds does not show any phase transition in the temperature range 1.5 – 730 K. Whereas the temperature dependence of the lattice parameter of $\text{BaMg}_{1/3}\text{Ta}_{2/3}\text{O}_3$ follows the classical expectations, the lattice parameter of relaxor ferroelectric $\text{PbMg}_{1/3}\text{Ta}_{2/3}\text{O}_3$ exhibits anomalies. One of these anomalies is observed in the same temperature range as the peak in the dielectric susceptibility. We find that in $\text{PbMg}_{1/3}\text{Ta}_{2/3}\text{O}_3$, lead ions are displaced from the ideal positions in the perovskite structure at all temperatures. Consequently short-range order is present. This induces strong diffuse scattering with an anisotropic shape in wavevector space. The temperature dependences of the diffuse neutron scattering intensity and of the amplitude of the lead displacements are similar.

PACS numbers: 77.80.-e, 61.12.-q

I. INTRODUCTION

Since complex $\text{AB}'_x\text{B}''_{1-x}\text{O}_3$ perovskites have two different ions in the B-sublattice, their properties are richer than the ones found in the classic ABO_3 counterparts¹. In particular, there is a subgroup of complex perovskites, relaxor ferroelectrics, which exhibit an anomaly in the dielectric susceptibility, broad in temperature and also frequency dependent. Unlike in usual ferroelectrics this anomaly does not link to macroscopic structural changes^{1,2}. Despite numerous studies, a coherent understanding of relaxor ferroelectrics is still lacking^{1,2,3,4,5}.

$\text{PbMg}_{1/3}\text{Nb}_{2/3}\text{O}_3$ (PMN) crystal is a model system to study relaxor behaviour^{1,2,6}. The real part of the dielectric permeability ϵ' of PMN has a maximum at $T \sim 270$ K and frequency $\nu = 10$ kHz¹. The average crystal structure of PMN is cubic down to 5 K⁷. However, an applied electric field induces a structural phase transition at $T \sim 210$ K⁸. $\text{PbMg}_{1/3}\text{Ta}_{2/3}\text{O}_3$ (PMT) is a well-known ferroelectric and it was among the first studied relaxors¹. The average structure is cubic in the range of examined temperatures and external electric fields^{1,9}. In PMT, the real part of the dielectric susceptibility at $\nu = 10$ kHz has a maximum at $T \sim 170$ K, *i.e.* considerably lower than in other important relaxor crystals like PMN and $\text{PbZn}_{1/3}\text{Nb}_{2/3}\text{O}_3$ (PZN)¹. This suggests that temperature-induced anharmonicity less affects the properties of PMT in the range of the dielectric anomaly. Consequently, PMT can be considered as the simplest relaxor system known. Thus, understanding the physical mechanisms underlying the relaxor properties in a PMT crystal should be easier than in the related compounds. Unfortunately, PMT was studied much less than PMN and PZN. It is only recently that

studies of PMT by X-ray diffraction^{9,10}, neutron scattering^{11,12,13,14}, light scattering^{12,15} and calorimetry¹⁶ were carried out. On the other hand, low-dielectric permeability is found in many Ba and Sr-based complex perovskites¹⁷. $\text{BaMg}_{1/3}\text{Ta}_{2/3}\text{O}_3$ (BMT) is an example of such a material¹⁸. In spite of chemical disorder in the B-sublattice, BMT does not exhibit any lattice instability or relaxor-like dielectric anomaly^{11,12,15,19}. Note also that exchanging lead in PMT with barium in BMT suppresses the relaxor properties of the former crystal. Thus, comparing the properties of PMT and BMT might be extremely instructive.

In this paper, we present results of neutron scattering studies in PMT and BMT in the temperature range $1.5 \text{ K} < T < 730 \text{ K}$, that covers the dielectric maximum¹ as well as the anomalies observed in the velocity and in the damping of the longitudinal acoustic phonon¹⁵ in PMT. In Section II, we describe the experimental procedure. Section III starts with the explanation of the different models used for the crystal structure refinement of PMT and BMT and contains a discussion of the diffuse scattering measurements in PMT. Further, in § III C, we present the temperature dependences of the lattice parameters of both BMT and PMT. In § IV A, we describe the evolution of the temperature factors and show that there is a pronounced correlation between the diffuse scattering intensity and the Pb displacements in PMT. In § IV B we propose a possible approach to describe DS in relaxors. Finally, in § IV C we compare the temperature dependences of the lattice parameter of PMT and PMN.

II. EXPERIMENTAL

The synthesis of the powder samples was described previously¹¹. The mass of each sample was about 15 grams. The single crystal of PMT used in the present study was grown by the Czochralski method and has a size $6.5 \times 4.5 \times 1.6 \text{ mm}^3$. The same crystal was used in previous dielectric, light and neutron scattering studies^{13,15}.

The measurements were performed at the neutron spallation source SINQ (PSI, Switzerland). The powder diffraction data were taken with the multi-detector high-resolution powder diffractometer HRPT²⁰. The polycrystalline samples of PMT and BMT were placed into cylindrical containers with 10 mm diameter and 50 mm height. Measurements were performed with the neutron wavelength $\lambda = 1.1545 \text{ \AA}$. This set-up gives access to more than 40 unique Bragg reflections in the range of scattering angles $7^\circ - 164.5^\circ$. A typical exposure time was ~ 20 minutes, but at few temperatures the exposure time was increased to ~ 4 hours. The program Fullprof²¹ was used for crystal structure refinement using the Rietveld method. The neutron scattering measurements on a single crystal of PMT were performed at the cold neutron three-axis spectrometer TASP²². The (002) reflection of pyrolytic graphite (PG) was used to monochromate and analyze the incident and scattered neutron beams. The PG monochromator was vertically curved and a PG filter placed in the incoming neutron beam was used to suppress contamination from higher-order neutron wavelengths. The spectrometer was operated in the elastic mode with the neutron wavevector $\mathbf{k}_i = 1.97 \text{ \AA}^{-1}$. The horizontal collimation was guide-80'-80'-80'. The sample was mounted on an aluminum holder with the (h h 0) and (0 0 l) Bragg reflections in the scattering plane.

III. RESULTS

A. Structure Refinement

Figure 1 shows the observed and calculated diffraction patterns obtained for BMT at $T=580 \text{ K}$. For the refinements, the chemical composition of $\text{BaMg}_{1/3}\text{Ta}_{2/3}\text{O}_3$ was fixed at the stoichiometric values. Random occupation of the Mg/Ta ions over the B-sites of BMT perovskite structure was assumed. In a first approach, we used anisotropic temperature factors for oxygen. It turned out, however, that within the statistical errors, the ratio $\beta_{11}/\beta_{33} \sim 1$ was constant even at high temperatures. Hence, for the subsequent refinements, the temperature factors were supposed to be isotropic. The crystal structure was found to be consistent with $\text{Pm}\bar{3}\text{m}$ space group, where barium is located at (0 0 0), oxygen is at (0.5 0.5 0), and Mg/Ta ions are statistically distributed over the (0.5 0.5 0.5) position. At $T = 580 \text{ K}$ the refinement procedure yielded a lattice constant $a = 4.10289(8) \text{ \AA}$ and temperature factors $B_{iso}(\text{Ba}) = 0.86(2) \text{ \AA}^2$, $B_{iso}(\text{O}) = 1.09(1) \text{ \AA}^2$,

$B_{iso}(\text{Mg}/\text{Ta}) = 0.60(1) \text{ \AA}^2$. This model gives a precise description of the experimental data ($\chi^2 = 2.52$, $R_p = 3.49$, $R_{wp} = 4.44$, $R_{Bragg} = 3.57$) and was used to refine neutron diffraction patterns at other temperatures. We note that, despite a general tendency toward hexagonal ordering in Ba-containing complex perovskites^{17,18}, the synthesis method described in Ref.¹¹ produces cubic perovskites with ionic disorder in the B-site.

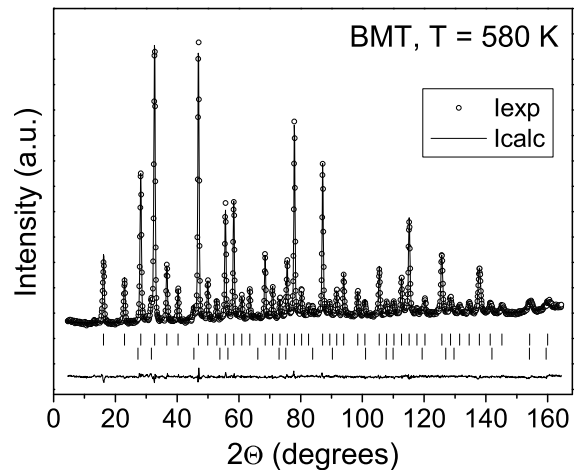


FIG. 1: Neutron powder diffraction pattern of BMT collected at $T = 580 \text{ K}$. Observed data points, calculated profile and difference curve are shown. The two rows of ticks correspond to the calculated positions of diffraction peaks for BMT (upper) and MgO impurity (3%).

Figure 2 shows the diffraction pattern obtained for PMT at $T=588 \text{ K}$ and treated with the Rietveld method. Different hypotheses for the structural model of PMT were tested during the refinement procedure. As in BMT, the cubic perovskite structure (space group $\text{Pm}\bar{3}\text{m}$) was assumed as a starting model. In this model, the refined values of the isotropic thermal parameters for lead and oxygen were found to be very high with $B_{iso}(\text{Pb}) = 4.08(3) \text{ \AA}^2$ and $B_{iso}(\text{O}) = 1.73(1) \text{ \AA}^2$, respectively. These values are much higher than those found for $B_{iso}(\text{Mg}/\text{Ta}) = 0.58(7) \text{ \AA}^2$, and for the isotropic temperature factors in the reference compound BMT. In particular, the large value of $B_{iso}(\text{Pb})$ is anomalous and indicates a possible structural disorder. A similar situation was observed before in many lead-based complex perovskites like PMN²³, PMN+ 10%PT (PMN-PT)²⁴, $\text{PbSc}_{1/2}\text{Nb}_{1/2}\text{O}_3$ ²⁵, and also in $\text{PbFe}_{1/2}\text{Nb}_{1/2}\text{O}_3$ ²⁶ (the list is far from complete). In all these examples, Pb was never found to be located exactly at the $1a$ (0 0 0) Wyckoff position. Thus, to improve our structural model, both displacements of Pb from the $1a$ (0 0 0) special Wyckoff position and anisotropic temperature factors for oxygen ions were introduced. We considered the shifts of Pb

along the $\langle 001 \rangle$, $\langle 110 \rangle$, and $\langle 111 \rangle$ directions.

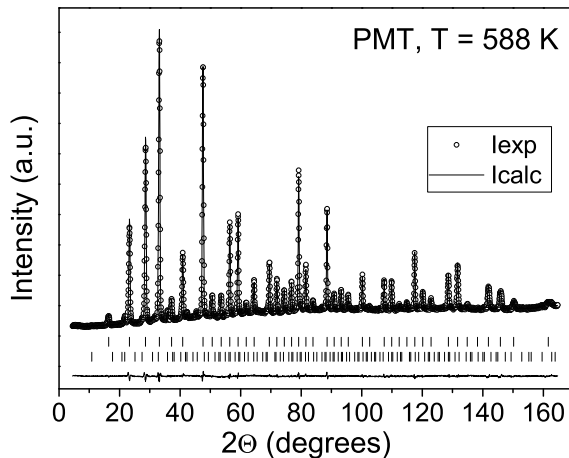


FIG. 2: Neutron powder diffraction pattern of PMT collected at $T = 588$ K. Observed data points, calculated profile and difference curve are shown. The two rows of ticks correspond to the calculated positions of diffraction peaks for perovskite PMT (upper) and pyrochlore impurity (5 %).

At 588 K the values for the Pb-shifts together with the reliability factors R_{Bragg} are tabulated in Table I. Reliability factors for Pb-shifts along the $\langle 001 \rangle$ direction are significantly worse than the corresponding value for the $\langle 110 \rangle$ and $\langle 111 \rangle$ directions. For the latter two directions, the quality of fit is nearly the same at all temperatures. Displacing Pb along $\langle 110 \rangle$ always gives a slightly better reliability factor and minimizes the value of the isotropic temperature factor of Pb. However, we do not put a strict physical sense in the choice of this particular direction for Pb-shifts. Namely, as was pointed out in Ref.²⁷, a preferable direction of the Pb-shifts can be artificial because of insufficiently high values in $(\sin \theta)/\lambda$ (note that we reached $(\sin \theta_{\max})/\lambda = 0.86 \text{ \AA}^{-1}$). To our opinion, the quality of refinement for the different displacement directions depends on the associated degeneracies: six-fold for the $\langle 001 \rangle$, eight-fold for $\langle 111 \rangle$ and twelve-fold for $\langle 110 \rangle$. The latter direction of shifts gives the closest approximation of a sphere. Hence, we used the $\langle 110 \rangle$ direction to refine the data taken at other temperatures.

To improve the structural model further, we introduced shifts for Mg/Ta ions and non-stoichiometric values for Pb and O content. However, the fit procedure converged to the nominal stoichiometric ratio. The introduction of shifts for Mg/Ta, while keeping all other parameters fixed, did not allow us to improve the structural model noticeably. Therefore, in the subsequent refinements, these parameters were fixed at their nominal values. The structural parameters obtained from the powder refinement at $T=588$ K are given in Table II. We ob-

TABLE I: Comparison between results of neutron powder refinement for different modeled directions of Pb shift at $T=588$ K in PMT.

Direction	Value (\AA)	$U_{iso}(\text{Pb})$ (\AA^2)	R_{Bragg}	χ^2
$\langle 001 \rangle$	0.27(0.05)	1.98(7)	3.76	3.63
$\langle 110 \rangle$	0.20(0.03)	1.51(6)	3.28	3.44
$\langle 111 \rangle$	0.16(0.04)	1.68(6)	3.35	3.47

TABLE II: Structural parameters for PMT obtained from refinement of data at $T = 588$ K. Space group: $\text{Pm}\bar{3}\text{m}$.

Parameters	Values
a (\AA)	4.05103(8)
Pb shift (\AA)	0.20(0.03)
Pb U_{iso} (\AA^2)	1.51(6)
Mg/Ta U_{iso} (\AA^2)	0.66(1)
O β_{11} (\AA) = β_{22} (\AA)	0.0340(3)
O β_{33} (\AA)	0.0101(4)
χ^2	3.44
R_p	2.88
R_{wp}	3.74

serve that on the contrary to BMT, the thermal ellipsoid for oxygen is anisotropic ($\beta_{11}/\beta_{33} \sim 3.44$). We note also that despite introduction of displacements, the isotropic temperature factor for Pb is still quite important (see Table I), being 2.5 times larger than $B_{iso}(\text{Mg/Ta})$ and 2 times larger than $B_{iso}(\text{Ba})$ in BMT.

B. Diffuse scattering

In the following, we discuss the influence of the diffuse scattering (DS) present on the powder diffraction pattern of PMT. Already in the earliest studies of PMN by X-rays²³ and neutron²⁸ diffraction, diffuse scattering was found, the intensity of which grows as the temperature decreases²⁸. Moreover, at low temperatures, DS is so strong that it becomes observable even in powder diffraction patterns²³. Later work on PMN single crystals showed that the distribution of diffuse scattering is anisotropic in reciprocal space^{29,30,31,32,33}. We have investigated the distribution of DS intensity in a single crystal of PMT at $T = 140$ K in the vicinity of the $(1\ 1\ 0)$ and $(0\ 0\ 1)$ Bragg positions. As shown in Fig. 3, the DS measured in the vicinity of $(1\ 1\ 0)$ Bragg peak of PMT has a "butterfly" shape in reciprocal space similar to the DS observed in single crystals of PMN³⁰. Note, that the intensity of DS is mainly concentrated along the equatorial section transverse to the $\langle 110 \rangle$ direction. Measurements in PMT around the $(0\ 0\ 1)$ Bragg peak give a very similar shape of DS. In that case, the most intense part

of diffuse scattering is concentrated along the equatorial section transverse to the $\langle 001 \rangle$ direction. It is obvious that the q -dependence of DS in PMT is complicated and to incorporate properly the DS into the structural model for powder refinement is an extremely difficult problem. Hence, the DS occurring in the powder diffraction pattern was treated as background.

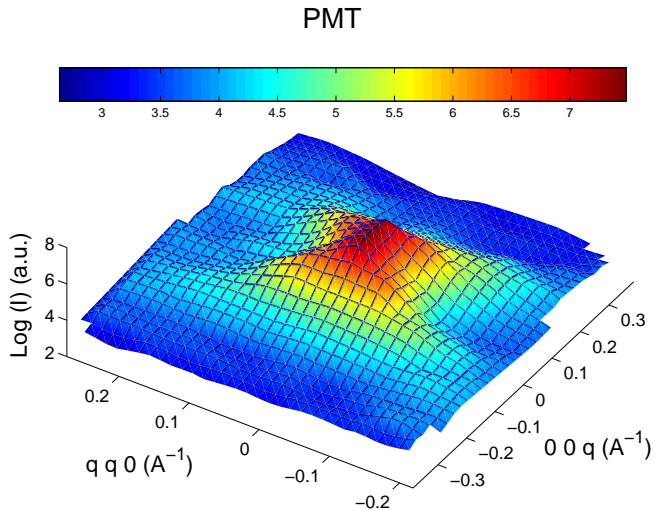


FIG. 3: Surface of neutron diffuse scattering intensity around the (110) Bragg peak of PMT at $T = 140$ K. Note that the intensity is given in a logarithmic scale.

C. Temperature dependence of the lattice parameters of PMT and BMT

Figure 4 shows that the temperatures dependences of the lattice parameters for BMT and PMT are qualitatively different. Starting from high temperature, the lattice parameter of BMT decreases almost linearly as the temperature decreases down to $T \sim 200$ K. There is a cross-over regime between this temperature and $T \sim 30$ K, below which the lattice parameter of BMT is approximately constant. The temperature dependence of the lattice parameter of BMT can be described by a quadratic polynomial $a_0 + a_{01} \times T + a_{02} \times T^2$, where $a_0 = 4.08275(8)\text{\AA}$, $a_{01} = 1.77(1) \cdot 10^{-5}\text{\AA} \cdot \text{K}^{-1}$ and $a_{02} = 2.6(1) \cdot 10^{-8}\text{\AA} \cdot \text{K}^{-2}$. Similar temperature dependences are commonly observed in solids (see for instance^{34,35} and references therein) and do not contain any signature of anomalies. This simply reflects that in a broad temperature range (1.5 K – 730 K), the lattice of BMT continuously expands. Hence, it appears that the presence of chemical disorder on the B-sublattice does not affect significantly the thermal expansion of the BMT lattice.

The variation of the lattice parameters of PMT can be separated into three distinct temperature regimes. As in BMT, the lattice parameter decreases linearly from high

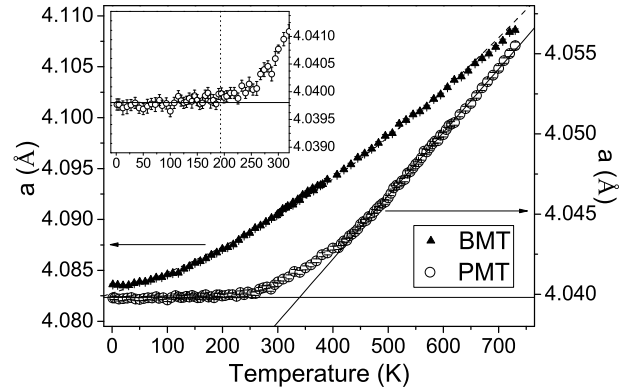


FIG. 4: Temperature dependence of the lattice parameters of PMT and BMT. The solid lines show the results of linear extrapolation for the $a(T)$ dependence of PMT. The dashed line shows the polynomial fit of $a(T)$ for BMT. The insert shows the dependence of the lattice parameter of PMT in the region of temperatures around $T \sim 180$ K. Invar-like behaviour of PMT for $T < 180$ K is obvious.

temperatures ($da(T)/dT = 3.8923 \cdot 10^{-5}\text{\AA} \cdot \text{K}^{-1}\text{T}$) with a cross-over regime between $T=420$ K and $T \sim 180$ K. Below this temperature, the lattice does not contract any more ($da(T)/dT = 8.8 \cdot 10^{-7}\text{\AA} \cdot \text{K}^{-1}$). On the contrary to what is observed for BMT, a quadratic polynomial does not reproduce the data shown in Fig. 4 and it is necessary to include powers up to 6 to describe the temperature dependence of the lattice parameter of PMT. It is clear that such a behaviour is anomalous. We remind the reader that the peak in the dielectric susceptibility of PMT appears around $T \sim 180$ K^{1,9}. Thus, the dielectric anomaly and the invar-like property in PMT are observed at the same temperature (see Insert of Fig. 4).

IV. DISCUSSION

A. Correlation between the diffuse scattering intensity and Pb displacements in PMT

We turn now to the description of the temperature dependence of the amplitude of Pb displacements ($\text{Pb}_{\langle XX0 \rangle}$) and of the DS intensity in PMT shown in Fig. 5. We measured the temperature dependence of the DS in PMT single crystal along $[1,1,q]$. In that direction, we find that the line-shape can be reproduced using a Lorentzian function¹³:

$$S(q) = \frac{I_0}{2\pi} \frac{\Gamma}{(q - q_0)^2 + \Gamma^2}, \quad (1)$$

where I_0 is the integrated intensity, Γ is the full width at half maximum (FWHM), and q_0 determines the center of the Lorentzian. Note that this approximation was

used in Ref.³² to analyze the intensity of DS in PMN. We monitored the evolution of DS in PMT in the temperature range 1.5 K – 375 K. At higher temperatures, the DS is extremely weak in intensity and broad in q -space, and the results obtained above $T \sim 400$ K cannot be analyzed reliably.

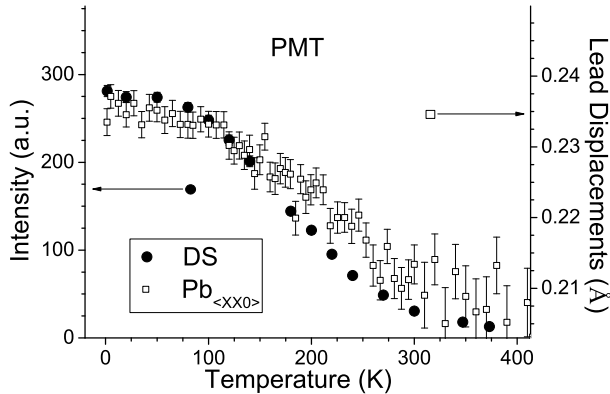


FIG. 5: Temperature dependences of the integrated intensity of diffuse scattering (DS) (black symbols) and amplitude of the Pb displacements ($Pb_{<XX0>}$) (open symbols) in PMT.

Figure 5 shows the temperature behaviour of the integrated intensity of DS and of the refined values of the $Pb_{<XX0>}$ shifts in the temperature range 1.5 – 412 K. Note that the values of the $Pb_{<XX0>}$ were derived from intensities of the Bragg peaks in the powder diffraction patterns whereas DS was extracted from the broad intensity distribution around these Bragg peaks *i.e.* from short-range correlations. The correlation length extracted from the FWHM of the DS line shape is found to increase continuously with decreasing temperature and was published previously¹³. There is a pronounced similarity between the increase of DS intensity and the displacement amplitude of $Pb_{<XX0>}$ as the temperature decreases. In the temperature range 1.5 K \sim 90 K both quantities are constant within statistical errors and decrease monotonously as the temperature is further increased. Finally, they tend to saturate above $T \sim 300$ K although a very slow decrease of $Pb_{<XX0>}$ above 412 K is not shown in Fig. 5 for better comparison with the DS intensity. The results shown in Fig. 5 strongly suggest that lead displacements may be responsible for the occurrence of DS in PMT. There is however no linear relationship between the temperature dependence of $Pb_{<XX0>}$ and DS: while the DS intensity decreases by a factor of ~ 30 when the temperature increases from 1.5 K to 375 K, the change in $Pb_{<XX0>}$ is of the order of $\sim 20\%$ only. At higher temperatures, lead displacements are still important, the DS is broad in q -space, since the correlation length is short¹³. In other words, while Pb displacements are *nearly uncorrelated* or *uncorrelated* the DS is weak (or totally absent). With decreasing temperature the

Pb displacements increase and become *correlated*, which causes the appearance of the DS. Note also, that one cannot claim that only Pb displacements are responsible for DS. However, it was possible to satisfactorily fit the diffraction patterns of PMT assuming that only lead ions are displaced. This suggests that the main contribution to the DS in relaxor crystals originates from Pb ions. The recent observation of a temperature-dependent relaxation mode, coexisting with the central peak in PMN crystal³⁶, also supports this hypothesis.

B. Possible description of the DS

We discuss now the resemblance observed for the temperature dependence of DS intensity and for $Pb_{<XX0>}$. It seems that the q -dependence of DS in all relaxors, which have been studied so far, is very similar. For example, DS with a "Butterfly-like" shape is observed in PMN^{32,33} and in PZN+8%PbTiO₃³⁷. Furthermore, the intensity of DS is found to increase with decreasing temperature in PMN^{24,28,32} and PZN^{38,39}, as here for PMT. From neutron and X-ray diffraction data, it is known that there is a general tendency that Pb displacements increase as the temperature decreases in complex perovskites (see *e.g.*^{7,25,27}). One can expect that the observed correlation between the DS intensity and the amplitudes of Pb displacements in PMT may help to create a model which describes short-range order in relaxors. In that vein, the calculations of Kassan-Ogly and Naish predicting an increase of diffuse scattering with decreasing temperature due to change in ionic-oscillation amplitudes may be considered as a useful starting point⁴⁰.

C. Lattice expansion

High-resolution neutron diffraction allowed us to study the temperature dependence of the lattice constant a in PMT from 41 unique Bragg reflections in the temperature range 1.5 K – 730 K with temperature step of ~ 10 K. We found changes of slope in $a(T)$ at ~ 420 K and ~ 180 K which do not strictly agree with previous temperature studies of the lattice parameters in PMT. In Ref.⁹, an anomaly was observed first at $T=573$ K and the lattice parameters were found to remain constant below $T=280$ K. We ascribe the discrepancy between our data and those by Lu *et al.*⁹ to the facts that, first, the latter measurements were carried out using three Bragg peaks of low Miller indices and, second, the number of temperature points was much reduced as compared to the present study. Thus, to our opinion there is no anomaly in the lattice parameter of PMT which could be directly connected with the Burns temperature $T_d \sim 570$ K⁴¹. Interestingly, the change of slope of $a(T)$ in PMT at high temperatures occurs at temperatures where we are able first to observe the diffuse scattering. In other words, deviation from linear law in $a(T)$ of PMT crystal appears

when the shifts of Pb ions become correlated. Note, that the so-called "excess" specific heat in PMT also appears at $T \sim 420$ K¹⁶.

It is useful to compare the behaviour of the lattice parameters of PMT and PMN^{7,24,46} in the temperature ranges where dielectric anomalies are observed. In the first neutron measurements by Husson *et al.*⁷, the lattice parameter of PMN was observed to remain roughly constant below $T \sim 300$ K. However, recent studies have revealed a more complicated behaviour of $a(T)$ in PMN. In Refs.^{24,46} a change of slope in $a(T)$ was found at $T \sim 350$ K and at $T \sim 200$ K. In the temperature range 200 – 350 K, Dkhil *et al.*²⁴ reported a freezing of the lattice parameters, similar to what we found in PMT below ~ 180 K. An important qualitative difference in the behaviors of the lattice parameters of PMN and PMT is that below $T \sim 200$ K, $a(T)$ for PMN decreases again as the temperature is lowered, whereas for PMT such a change of regime is absent. We remind that at $T \sim 210$ K PMN has an additional phase transition in an applied electric field⁸. However, even without application of an external electric field, properties like damping of longitudinal acoustic phonons⁴⁴, and the width of quasielastic component in light scattering spectra⁴⁵ exhibit anomalies in PMN in the vicinity of this temperature. Thus, it is possible that this lattice instability is linked with the additional change of $a(T)$ of PMN as the temperature decreases below 200 K.

In the following we discuss possible causes for the anomalous temperature dependence of the lattice parameter in PMT. As it is well-known (see for instance⁴⁷), the unit cell volume V depends on temperature T as

$$\frac{dV}{V} = \frac{\kappa_T C_V}{V} \gamma(T, V) dT, \quad (2)$$

where κ_T is the isothermal compressibility, $\gamma(T, V)$ the Grüneisen function, and C_V the heat capacity taken at constant volume. However, it is not easy to understand the low-temperature saturation of $a(T)$ below the temperature of the maximum in ε' . The problem is related to the large number of observed anomalies in the vibration spectra of PMT (as well as in other relaxors) for temperatures close to the dielectric maximum, like

- increase in the generalized density of states at low energies^{11,12},
- anomalies in the behaviour of the longitudinal acoustic phonons^{15,43},
- excess contribution to the specific heat^{16,48}.

Hence, to estimate the influence of each of this anomalies on the behaviour of $a(T)$ using *e.g.* Eq. (2) is an extremely complicated problem. We note only that an invar-like behaviour generally can be described *e.g.* by compensation of anharmonic behaviour of different phonon modes⁴⁹ or striction. The electrostriction mechanism originally proposed in Ref.² can also give some contribution in the behaviour of $a(T)$. Since $a(T)$ is linear at temperatures well below T_d , it is unlikely that electrostriction is the only mechanism responsible for the temperature evolution of the lattice parameters in PMT.

V. CONCLUSION

To summarize, an extensive neutron study has been carried out in PMT and BMT complex perovskites in the temperature range 1.5 K – 730 K. The surface of diffuse scattering in a PMT single-crystal has been measured at $T = 140$ K. Crystal structure parameters have been refined for both compounds. We found that lead ions are shifted from the $1a$ (0 0 0) Wyckoff position of the ideal perovskite structure and that the thermal motion parameter of oxygen is anisotropic in PMT. The lattice parameter of BMT does not exhibit any anomalous behaviour. On the other hand, the lattice parameter of PMT shows two anomalies. One of them appears around $T = 420$ K which corresponds to the appearance of diffuse scattering and of the excess specific heat in PMT. The second anomaly is found close to the maximum of the dielectric susceptibility at $T = 180$ K. An obvious correlation in the behaviour of the lead displacements and of the neutron diffuse scattering intensity is observed in PMT. This indicates that lead displacements play a major rôle in the occurrence of diffuse scattering in PMT and probably also in other relaxor ferroelectrics.

Acknowledgments

The authors would like to thank Dr. P. Fischer for useful discussions and N.V. Zaitzeva for X-rays characterization of powder samples. This work was performed at the spallation neutron source SINQ, Paul Scherrer Institut, Villigen (Switzerland) and was partially supported by RFBR Grant No. 02-02-17678 and by Grant of President RF ss-1415.2003.2.

* On leave from Ioffe Physical Technical Institute, 26 Politekhnicheskaya, 194021, St. Petersburg, Russia

¹ G.A. Smolenskii, V.A. Bokov, V.A. Isupov, N.N. Krainik, R.E. Pasyukov, N.K. Yushin, *Ferroelectrics and Related*

Materials (New York, Gordon and Breach, 1984).

² L.E. Cross, *Ferroelectrics* **76**, 241 (1987).

³ V. Westphal, W. Kleemann, M.D. Glinchuk, *Phys. Rev. Lett.* **68**, 847 (1992).

- ⁴ D. Viehland, S.J. Jang, L.E. Cross, M. Wuttig, Phys. Rev. B **46**, 8003 (1992).
- ⁵ R. Blinc, J. Dolinsek, A. Gregorovic, B. Zalar, C. Filipic, Z. Kutnjak, A. Levstik, R. Pirc, Phys. Rev. Lett. **83**, 424 (1999).
- ⁶ I.G. Siny, S.G. Lushnikov, R.S. Katiyar, V.H. Schmidt, Ferroelectrics **226**, 191 (1999).
- ⁷ P. Bonneau, P. Garnier, G. Calvarin, E. Husson, J.R. Gavarri, A.W. Hewat, A. Morell, J. Solid State Chem. **91**, 350 (1991).
- ⁸ G. Schmidt, H. Arndt, J. Voncieminski, T. Petzsche, H. Voigt, N. Krainik, Krist. und Tech. **15**, 1415 (1980).
- ⁹ Z.G. Lu, C. Flicoteaux, G. Calvarin, Materials Research Bull. **31**, 445 (1996).
- ¹⁰ M.A. Akbas, P. Davies, J. Am. Ceram. Soc. **80**, 2933 (1997).
- ¹¹ S.N. Gvasaliya, S.G. Lushnikov, I.L. Sashin, T.A. Shaplygina, J. Appl. Phys. **94**, 1130 (2003).
- ¹² S.N. Gvasaliya, S.G. Lushnikov, I.L. Sashin, Ferroelectrics **285**, 617 (2003).
- ¹³ S.N. Gvasaliya, B. Roessli, S.G. Lushnikov, Europhys. Lett. **63**, 303 (2003).
- ¹⁴ S.N. Gvasaliya, S.G. Lushnikov, B. Roessli, Crystallogr. Rep. **49**, 108 (2004).
- ¹⁵ Jae-Hyeon Ko, S. Kojima, S.G. Lushnikov, Appl. Phys. Lett. **82**, 4128 (2003).
- ¹⁶ Yosuke Moriya, Hitoshi Kawaji, Takeo Tojo, Toru Atake, Phys. Rev. Lett. **90**, 205901 (2003).
- ¹⁷ F.F. Galasso *Structure, properties and preparation of perovskite-type compounds* (Pergamon Press, Oxford, UK, 1969).
- ¹⁸ A.S. Bhalla, R. Guo, I.G. Siny, R. Tao, R.S. Katiyar, J. Phys. Chem. Solids **59**, 181 (1998).
- ¹⁹ R. Guo, A.S. Bhalla, L.E. Cross, J. Appl. Phys. **75**, 4704 (1994).
- ²⁰ P. Fischer *et al.*, Physica B **276&278**, 146 (2000).
- ²¹ J. Rodríguez-Carvajal, Physica **192B**, 55 (1993).
- ²² P. Böni, P. Keller, Proceedings of the 4th Summer School on Neutron Scattering, Zuzo, Switzerland, August 18-24, 1996, PSI-Proceedings 96-02 35-42 (1996).
- ²³ N. de Mathan, E. Husson, G. Calvarin, J. R. Gavarri, A. W. Hewat, A. Morell, J. Phys.: Condens. Matter. **3**, 8159 (1991).
- ²⁴ B. Dkhil, J.M. Kiat, G. Calvarin, G. Baldinozzi, S.B. Vakhrushev, E. Suard, Phys. Rev. B **65**, 024104 (2002).
- ²⁵ C. Malibert, B. Dkhil, J.M. Kiat, D. Durand, J.F. Berar, A. Spasojevic-de-Biré, J. Phys.: Condens. Matter **9**, 7485 (1997).
- ²⁶ N. Lampis, P. Sciau, A.G. Lehmann, J. Phys.: Condens. Matter **11**, 3489 (1999).
- ²⁷ S.B. Vakhrushev, S.G. Zhukov, G.V. Fetisov, V.V. Chernyshov, J. Phys.: Condens. Matter **6**, 4021 (1994).
- ²⁸ S.B. Vakhrushev, B.E. Kvyatkovsky, A.A. Nabereznov, N.M. Okuneva, B.P. Toperverg, Ferroelectrics **90**, 173 (1989); S.B. Vakhrushev, B.E. Kvyatkovsky, A.A. Nabereznov, N.M. Okuneva, B.P. Toperverg, Physica **B156-157**, 90 (1989).
- ²⁹ S.B. Vakhrushev, A.A. Nabereznov, N.M. Okuneva, B.N. Savenko, Phys. Solid State **37**, 1993 (1995).
- ³⁰ K. Hirota, Z.-G. Ye, S. Wakimoto, P.M. Gehring, G. Shirane, Phys. Rev. B **65**, 104105 (2002).
- ³¹ B. Chaabane, J. Kreisel, B. Dkhil, P. Bouvier, M. Mezouar, Phys. Rev. Lett. **90**, 257601 (2003).
- ³² Guangyong Xu, G. Shirane, J.R.D. Copley, P.M. Gehring, Phys. Rev. B **69**, 064112 (2004).
- ³³ H. You, Q. M. Zhang, Phys. Rev. Lett. **79**, 3950 (1997).
- ³⁴ H.P. Singh, G. Simmons, P.F. McFarlin Acta Cryst. **A31**, 820 (1975).
- ³⁵ Fei, Y. (1995). AGU Reference Shelf 2: Mineral Physics and Crystallography, A Handbook of Physical Constants, edited by T. J. Ahrens, pp. 29-44. Washington: AGU.
- ³⁶ S.N. Gvasaliya, S.G. Lushnikov, B. Roessli, Phys. Rev. B **69**, 092105 (2004).
- ³⁷ J. Hlinka, S. Kamba, J. Petzelt, J. Kulda, C.A. Randall, S.J.Zhang, J. Phys.: Condens. Matter **15**, 4249 (2003).
- ³⁸ D. La-Orauttapong, J. Toulouse, J.L. Robertson, Z.-G. Ye Phys. Rev. B **64**, 212101 (2001).
- ³⁹ C. Stock, R.J. Birgeneau, S. Wakimoto, J.S. Gardner, W. Chen, Z.-G. Ye, G. Shirane, Phys. Rev. B **69**, 094104 (2003).
- ⁴⁰ F.A. Kassar-Ogly, V.E. Naish, Acta Cryst. **B42**, 297 (1986); Acta Cryst. **B42**, 307 (1986); Acta Cryst. **B42**, 314 (1986); Acta Cryst. **B42**, 325 (1986).
- ⁴¹ G. Burns *et al.* have measured the refraction index of PMN, PZN and $\text{Pb}_{1-x}\text{La}_x(\text{Zr}_{0.65}\text{Ti}_{0.35})_{1-x/4}\text{O}_3$ ⁴², but to the best of our knowledge, the refraction index of PMT was never measured. Therefore, to determine the Burns temperature T_d in PMT we rely on Brillouin light scattering data¹⁵. In the case of PMN the value of T_d extracted from Brillouin data⁴³ is in reasonable agreement with the original papers of G. Burns *et al.*⁴². We believe that this is the case also for PMT.
- ⁴² G. Burns, B.A. Scott, Solid State Communications **13**, 423 (1973).
- ⁴³ S.G. Lushnikov, J.-H. Ko, S. Kojima, Ferroelectrics (2004) (in press).
- ⁴⁴ R. Laiho, S.G. Lushnikov, I.G. Siny, Ferroelectrics **125**, 493 (1992).
- ⁴⁵ I.G. Siny, S.G. Lushnikov, R.S. Katiyar, E.A. Rogacheva Phys. Rev. B **56**, 7962 (1997).
- ⁴⁶ C.N.W. Darlington, W.I.F. David, K.S. Knight, K.A. Müller, ISIS Experimental Report RB7765, (1997).
- ⁴⁷ T.H.K. Barron, G.K. White, *Heat Capacity and Thermal Expansion at Low Temperatures* (Kluwer Academic/Plenum Publishers, New York, 1999).
- ⁴⁸ S.N. Gvasaliya, S.G. Lushnikov, Y. Moriya, H. Kawaji, T. Atake, M.B. Smirnov, V.Yu. Kazimirov, (to be published).
- ⁴⁹ G. Grimvall in *Thermophysical properties of materials* (North-Holland/Elsevier, Amsterdam, 1999).